

# Controlling the quantum number distribution and yield of Rydberg states via the duration of the laser pulse

L. Ortmann<sup>1,\*</sup>, C. Hofmann<sup>1</sup>, and A. S. Landsman<sup>1,2†</sup>

<sup>1</sup>*Max Planck Institute for the Physics of Complex Systems,  
Nöthnitzer Straße 38, D-01187 Dresden, Germany*

<sup>2</sup>*Department of Physics, Max Planck Postech, Pohang, Gyeongbuk 37673, Republic of Korea*

(Dated: December 15, 2024)

We show that the distribution of quantum numbers of Rydberg states does not only depend on the field strength and wavelength of the laser which the atom is exposed to, but that it also changes significantly with the duration of the laser pulse. We provide an intuitive explanation for the underlying mechanism and derive a scaling law for the position of the peak in the quantum number distribution on the pulse duration. The new analytic description for the electron's movement in the superposed laser and Coulomb field (applied in the study of quantum numbers) is then used to explain the decrease of the Rydberg yield with longer pulse durations. This description stands in contrast to the concepts that explained the decrease so far and also reveals that approximations which neglect Coulomb effects during propagation are not sufficient in cases such as this.

## I. INTRODUCTION

If the field strength of a laser field is comparable to the Coulomb force of an atom, the laser field can bend the Coulomb potential so strongly that a barrier is formed through which an electron can tunnel out of the atom [1–3]. After this, the electron does not necessarily leave the atom for good, but can get captured in a Rydberg state, thus creating neutral excited atoms [4, 5].

The relevance of this effect, which is often referred to as ‘frustrated tunnel ionization’ (FTI), already becomes clear by the observation that in typical strong field systems 10-20% of tunnel ionized electrons are trapped in Rydberg states [4], thus affecting many more electrons than other post-tunnel ionization mechanisms such as HHG or double ionization by collision, which typically involves a much smaller fraction of electrons [6, 7]. FTI does not only explain the significant reduction of ionization rates [4], but can also be used to e.g. calibrate laser intensities [8], study nonadiabatic effects [9], probe the spatial gradient of the ponderomotive potential in a focused laser beam [10], or control the motion of neutral atoms in strong laser fields [7, 11].

Rydberg states populate different quantum numbers, the distribution of which is important for the characterization of the excited neutral Rydberg atoms, e.g. in terms of their lifetime before decaying into metastable states [4]. Recently, the distribution of principle quantum numbers has helped understand e.g. the stability of excited states under the influence of a second laser pulse [7, 8], ionization channels and their closings [12, 13] as well as the effect of spatial gradients in the laser field [14].

It has been observed that the principal quantum numbers shift to higher values for larger intensities and larger

wavelengths of the laser pulse [15–18]. In this work, after introducing the basic equations and concepts of Rydberg states in section II, we will investigate the effect that the pulse duration of the laser has on the distribution of quantum numbers in section III. The insights gained in the study of the quantum number distribution will then be used to understand the dependence of the fraction of atoms that end up in a Rydberg state on pulse duration.

## II. BASIC EQUATIONS

We assume that the laser field that the atoms are exposed to is linearly polarized in  $z$ -direction and can be described as follows:

$$\vec{E}(t) = \mathcal{E}_0 \cos(\omega t) \cos^2\left(\frac{\omega t}{2N}\right) \vec{e}_z, \quad (1)$$

with the maximal field strength  $\mathcal{E}_0$ , the laser frequency  $\omega$  and the total number of optical cycles  $N$ . Note that throughout the paper we will use atomic units, unless stated otherwise. An electron that leaves the atom will feel the Coulomb potential even after its liberation and will be captured in a bound state, provided the kinetic energy is sufficiently small after the laser pulse has passed, such that the total energy is negative [5]:

$$E = \frac{v^2}{2} - \frac{1}{r} < 0. \quad (2)$$

Even though there are quantum effects in Rydberg states that can only be explained invoking the time-dependent Schrödinger equation [19], it has been found that an electron captured in a Rydberg state can be well described by the motion on a classical Kepler orbit around the parent ion after the laser pulse has passed and that in this framework and following Bohr's model we can assign principle quantum numbers to that Rydberg state given by [5, 20],

$$E = -\frac{0.5}{n^2} \quad (3)$$

\* ortmann@pks.mpg.de

† landsman@pks.mpg.de

where the factor of 0.5 is the Rydberg constant.

As semiclassical simulations have been found to be a powerful tool for understanding phenomena related to Rydberg atoms [21–23], we use a Classical Trajectory Monte Carlo simulations (CTMC) method for our study with ADK probability for the initial conditions [24, 25]:

$$P_{ADK}(t_0, v_{\perp,0}) \approx \exp \left( -\frac{2(2I_p(t_0))^{3/2}}{3\mathcal{E}(t)} \right) \cdot \exp \left( -\frac{v_{\perp,0}^2(2I_p(t_0))^{1/2}}{\mathcal{E}(t)} \right) \quad (4)$$

with  $t_0$  denoting the time of the electron's appearance at the tunnel exit and  $v_{\perp,0}$  being its initial velocity perpendicular to the laser polarization. For a detailed description of the method we refer to [26]. The coordinates of the tunnel exit are calculated on the basis of the energy conservation law in parabolic coordinates [27–29]. The electron trajectories are then propagated in the superposed potential of the laser and Coulomb field solving Newton's equations:

$$\ddot{\vec{r}} = -\vec{\mathcal{E}}(t) - \frac{\vec{r}}{(\vec{r}^2 + a^2)^{3/2}}. \quad (5)$$

with soft core parameter  $a^2 = 0.01$ .

### III. THE QUANTUM NUMBER DISTRIBUTION

Prior simulations show that the principal quantum number of Rydberg states increases with laser intensity and wavelength [15–18]. This has previously been explained by invoking the following dependence [5, 16]:

$$n \approx \frac{\sqrt{\mathcal{E}_0}}{\omega}. \quad (6)$$

The above relation can be understood by considering the virial theorem, which gives a relation between the time-averaged kinetic and potential energy for a motion in a Coulomb potential

$$\begin{aligned} \bar{T} &= -\frac{1}{2}\bar{U} \\ \Rightarrow \bar{E} &= \bar{T} + \bar{U} = \frac{1}{2}\bar{U} = -\frac{0.5}{\langle r \rangle} = -\frac{0.5}{n^2} \\ \Rightarrow n &= \sqrt{\langle r \rangle} \end{aligned} \quad (7)$$

where we used eq. (3) to obtain the last line. Assuming that the average position can be approximated by the quiver amplitude  $\mathcal{E}_0/\omega^2$  of the electron in the laser field one obtains eq. (6).

However, our CTMC simulations reveal that the distribution of principle quantum numbers also depends on the pulse duration, as can be seen in Fig. 1. This result shows that the quantum number distribution in general

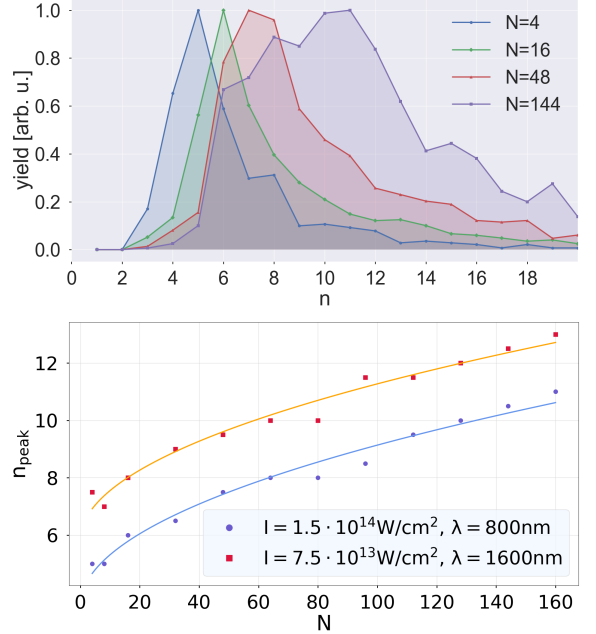


FIG. 1. Top panel: Distribution of principal quantum numbers for various pulse durations specified by the number of cycles  $N$  in the legend. The result was obtained for ionization of hydrogen at a laser intensity of  $I = 1.5 \cdot 10^{14} \text{ W/cm}^2$  and the wavelength is  $\lambda = 800 \text{ nm}$ . Bottom panel: The dots give the position of the peak in the distribution of the principle quantum number vs. the pulse duration. Note that in cases where the peak is not clearly found at a single  $n$  value, as it is e.g. the case for  $N = 144$  in the top panel, we averaged over the  $n$  values at which the peak appears. The lines represent fits according to eq. (8). The results were obtained for ionization of hydrogen at two different laser parameters that are specified in the legend.

and its peak in particular shift to larger  $n$  for longer pulse durations. The fit to the data presented in the bottom panel of Fig. 1 suggests that the peak of the principle quantum number distribution grows like  $\sqrt{N}$ .

Before trying to understand the reason for that scaling, we want to obtain a qualitative and intuitive understanding for the growth of  $n$  with increasing pulse duration. To this end, we look at a map of the initial conditions - the ionization time  $t_0$  and the initial transverse velocity  $v_{t,0}$  at the tunnel exit - on the final energy, which can be directly converted into the principle quantum number  $n$  using eq. (3). Such maps can be found in Fig. 2 for various pulse durations. First of all, they show that the area the Rydberg states are found in is crescent-shaped with the smaller principle quantum numbers located at the inner edge with  $n$  increasing towards the outer edge of the crescent. This makes sense as the earlier and thus farther away from the field maximum the electron is born, the more it is accelerated. Consequently, at the outer edge of the crescent we find electrons with a large kinetic energy due to acceleration in the laser or due to a large initial velocity, thus the total energy is higher (less negative)

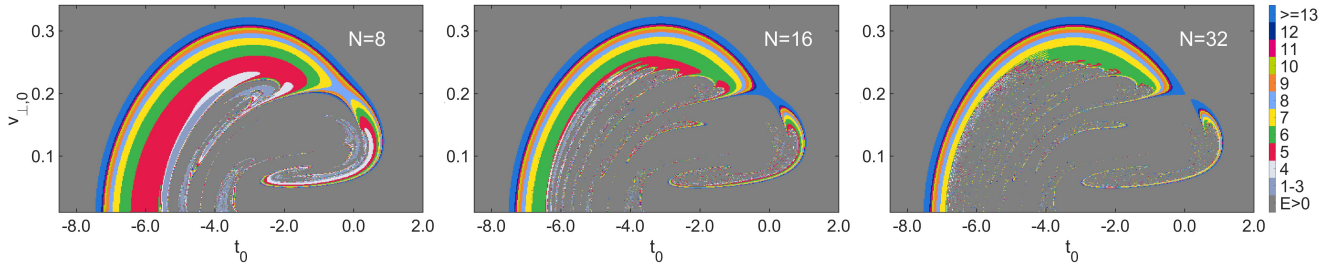


FIG. 2. Map of the principal quantum number  $n$  depending on the ionization time  $t_0$  and the initial transverse velocity  $v_{\perp,0}$ . Initial conditions which do not end up in a Rydberg state (positive total energy,  $E > 0$ ) are marked in gray. The pulse duration is given by the number of cycles  $N$  in the plots and increases from left to right. The increasing pulse duration leads to the crescent-shaped Rydberg area waning from the inside.

in the outer region of the crescent, which corresponds to large principle quantum numbers according to equation (3).

More importantly, Fig. 2 reveals that the position of the quantum numbers in the crescent does not change with the pulse duration, but that for increasing pulse duration the inner part of the crescent ceases to be part of the ‘Rydberg area’, which we define as the area in the plane of initial conditions  $(t_0, v_{t,0})$  that corresponds to electron capture into a Rydberg state. Tracking single electron trajectories reveals that electrons that get trapped into Rydberg orbits for a short pulse duration but not for a longer one, at some point strongly interact with the Coulomb field of the residual ion, thus gaining sufficient kinetic energy to escape the parent ion. In some rare cases, found in the stripes in the center of the crescent, these ‘recolliding’ electrons will still end up in a Rydberg state (see for example  $t_0 = -4$  for small initial transverse velocities for  $N = 8$  in Fig. 2).

To conclusively establish that the loss of Rydberg electrons for longer pulses (occurring for initial conditions corresponding to the inner region of the crescent) is caused by the longer time in the laser field, rather than a particular shape of the laser pulse, we perform additional simulations. We find that in cases with a constant envelope, meaning we replace the  $\cos^2$  term in eq. (1) by a heaviside step function with a constant non-zero value in the interval  $[-N/2, N/2] \cdot 2\pi/\omega$ , we obtained almost the same crescents as the ones with the  $\cos^2$  envelope shown in Fig. 2, with significant discrepancies only for very small pulse durations in the regime of  $N \leq 4$ . This shows that the key reason for Rydberg states being ‘scattered out of the crescent’ for longer pulse durations is the long time the electrons spend in the laser field rather than the particular envelope shape.

This is further corroborated by Fig. 3, which shows single trajectories around the inner edge of the crescent for two different pulse durations - one that still allows the electron to end up in a Rydberg state ( $N = 16$ ) and the other one having one more optical cycle ( $N = 17$ ) during which the electron then interacts strongly with the Coulomb field gaining a considerable amount of ki-

netic energy. In the central panel of Fig. 3 we can see that the electron position oscillates around a parabola shaped curve - which in the first optical cycles of propagation leads to the electron going further away from the residual ion and coming closer to it later on. If the pulse duration is sufficiently long, the electron comes back to the ion and ‘recollides’. As the parabola that the position oscillates around is crucial and not so much the amplitude of the oscillation itself, which would be reduced by a  $\cos^2$  envelope, we can understand why the shape of the envelope is not as important as the duration of the pulse.

How can we understand that the electron’s position along the laser polarization axis oscillates around a parabola? This is directly linked to the approximately linear positive slope function that the velocity  $v_z(t)$  oscillates around (see bottom panel of 3). The positive slope is, in turn, due entirely to the pull of the Coulomb potential in the direction of the residual ion (see appendix A for details).

As indicated by the lines in the bottom panel of Fig. 1, we find that the principal quantum number  $n$  peaks at values  $n_{peak}$  that can be fitted by the following function

$$n_{peak} = A + B\sqrt{N} \quad (8)$$

with fitting parameters  $A$  and  $B$ . We can understand that the increase scales with  $\sqrt{N}$  by looking at the parabola that  $z$  oscillates around. As described at the beginning of this section, we expect  $n \propto \sqrt{\langle r \rangle}$  (see eq. (7)). We define  $N_{max}$  as the maximal number of cycles in the pulse that sill leads to a Rydberg state ( $N_{max} = 16$  in the example presented in Fig. 3) - it is directly linked to the zero-crossing of the parabola and its value depends strongly on the initial conditions  $(t_0, v_{t,0})$ . Now, we find that  $N_{max}$  is proportional to the extreme value of the parabola, which we call  $z_{max}$ , (see appendix B for details). As a consequence, also the mean elongation  $\langle z \rangle$  of the parabola depends approximately linearly on  $N_{max}$ . Also the motion transverse to the polarization axis happens along a parabola and an analogous line of reasoning can be applied here. Therefore, we obtain  $n \propto \sqrt{\langle r \rangle} \propto \sqrt{N_{max}}$ . As the maximal number of cycles  $N_{max}$  defines the inner edge of the crescent and also

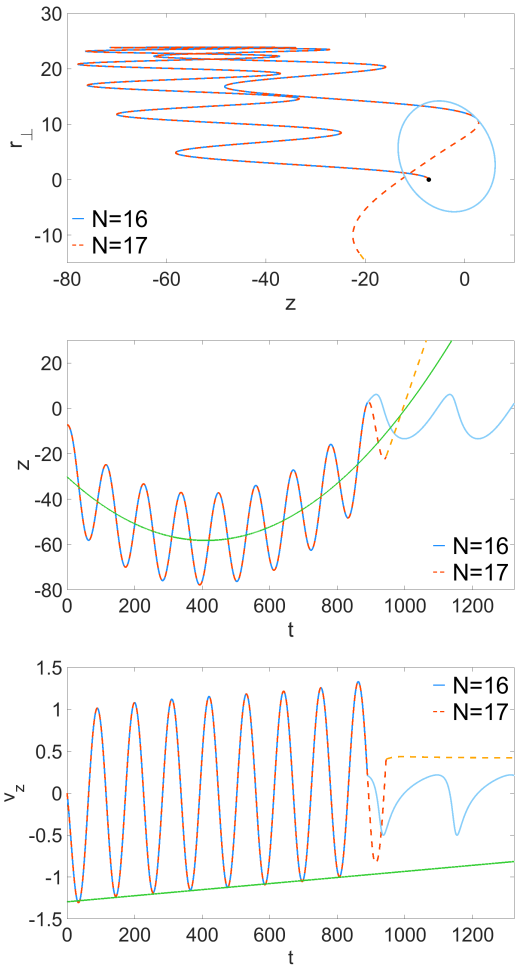


FIG. 3. Data for trajectories released at  $t_0 = -6.4$  and  $v_{\perp,0} = 0.09$  from a hydrogen atom and propagated in a laser field with  $I = 1.5 \cdot 10^{14} \text{ W/cm}^2$  and  $\lambda = 800 \text{ nm}$  that has a constant envelope with a total number of cycles  $N = 16$  and  $N = 17$ , respectively. Note that as the electron is released in the central cycle it experiences only about half of the total number of cycles in the pulse. a) Coordinates  $z$  and  $r_{\perp} = \sqrt{x^2 + y^2}$  for the trajectories during the propagation in the laser pulse and slightly afterwards. b) and c) show the position  $z$  and velocity  $v_z$  along the polarization axis as a function of propagation time, respectively. After the pulse is over the color of the respective trajectory is displayed in a lighter shade of the color that it had while the pulse was still on.

the most likely  $n$  value, we can replace  $N_{max}$  by  $N$  and obtain eq. (8).

#### IV. FRACTION OF RYDBERG STATES

The pulse duration not only affects the quantum number distribution, but also influences strongly the fraction of electrons that end up in a Rydberg state. Using CTMC simulations for various intensities and pulse durations, we

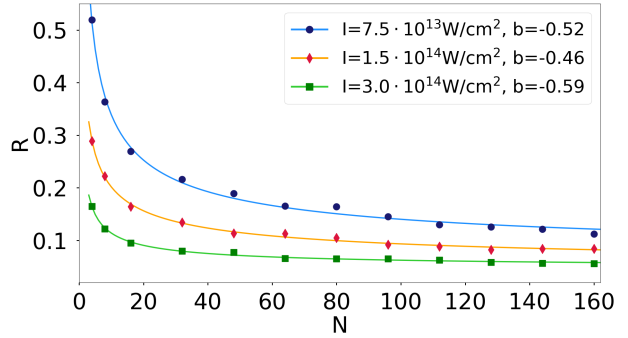


FIG. 4. The dots represent the numerically obtained Rydberg ratio  $R$ , defined as the number of electrons that end up in a Rydberg state divided by the number of all electrons that tunneled out of the atom, as a function of the pulse duration encoded in the number of cycles  $N$  for ionization from a hydrogen atom in a laser field as defined by eq. (1) at a wavelength of  $\lambda = 800 \text{ nm}$  for three different intensities that are specified in the legend. The solid lines represent the fit results using the function given in eq. (9), where the crucial fitting parameter  $b$  is given in the legend.

find a dependence on the pulse duration,  $\tau$ , (see Fig. 4) in approximate agreement with prior findings [4, 5] which gave a  $\tau^{-2/3}$  dependence. Here, we define the Rydberg ratio  $R$  as the number of electrons that end up in a Rydberg state divided by the number of all electrons that tunneled out of the atom. We fit the Rydberg ratio as a function of the pulse duration, which is encoded in the number of cycles  $N$ , by a function

$$R(N) = a \cdot N^b + c \quad (9)$$

with fitting parameters  $a$ ,  $b$  and  $c$  and find that  $b \approx -0.5$  in all cases. This confirms prior numerical results [5], but offers a different explanation that crucially relies on the previously neglected Coulomb potential during propagation.

Prior treatments neglected the Coulomb potential, which was viewed as a higher-order correction, during propagation [5, 22]. Only after the pulse was over, the Coulomb potential was accounted for by evaluating eq. (2) [5]. In this framework, it was found that the minimal ionization time and the maximal transverse velocity that lead to a Rydberg state (which define the limit of  $E = 0$  in eq. (2) and mark the outer edge of the crescent-shaped Rydberg area) decrease with longer pulse duration. Following this line of reasoning, the Rydberg area in the plane spanned by the ionization time  $t_0$  and the initial transverse velocity  $v_{t,0}$  shrinks because the outer borders of the Rydberg area depend on the propagation time. This, however, stands in contrast to what we find numerically. As is shown in Fig. 2, the Rydberg area indeed shrinks with longer pulse duration, but the outer boundaries of the crescent stay more or less constant for all pulse durations, while the Rydberg states vanish from the inner part of the crescent for longer pulse durations. Thus, we see that the limit of  $E = 0$  in eq. (2)

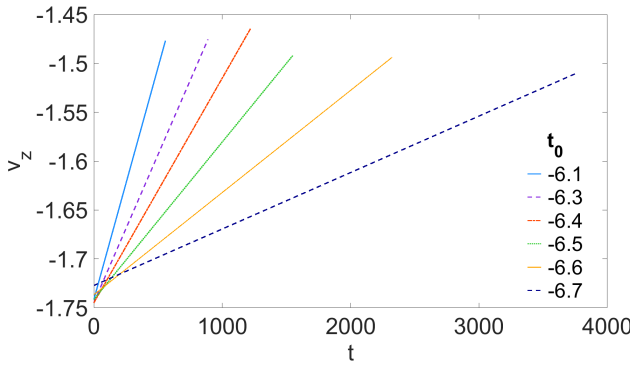


FIG. 5. Linear fit to the minima of  $v_z$  obtained for ionization from hydrogen at a laser intensity of  $I = 3.0 \cdot 10^{14} \text{ W/cm}^2$ , a wavelength of  $\lambda = 800\text{nm}$  and a initial transverse velocity  $v_{t,0} = 0.15$  for different ionization times  $t_0$ . The pulse duration differs in each case and is chosen such that one optical cycle more would cause a strong Coulomb interaction that accelerates the electron such that it will not be captured in a Rydberg state.

is hardly affected by the pulse duration, but that those electrons that end up at more negative energies have a higher chance of recolliding and therefore ionizing during longer pulse durations. As this effect is just what we used in our explanation of the change in the quantum number distribution, it allows us to understand the decrease of the Rydberg ratio qualitatively by the arguments given in section III. Moreover, we can directly conclude that we need to go beyond the approximation of neglecting the Coulomb force during the electron's propagation while the pulse is on to understand the decrease of the Rydberg ratio with longer pulse duration.

In order to understand the drop of the Rydberg ratio by about  $1/\sqrt{N}$ , we assume that the crescent-shaped Rydberg area in the central cycle of the pulse is proportional to the number of Rydberg states [5]. The underlying approximation here is that the ionization rate is constant over the ionization time in question, which is justified by the fact that the ionization times that potentially lead to a Rydberg state are found in a rather small time range. Furthermore, as shown in Appendix C (see also [5]), the size of the crescent shaped Rydberg area can be assumed to be proportional to the boundaries of the area in the  $t_0$  direction:

$$R \propto (t_{0,max} - t_{0,min}), \quad (10)$$

where  $t_{0,min}$  is the minimal initial time that leads to a Rydberg state and that is independent of the pulse duration and  $t_{0,max}$  defines the pulse duration dependent maximal initial time that leads to a Rydberg state.

When the pulse is sufficiently long so that the total area under the  $v_z$  curve, which corresponds to the position of the electron, becomes approximately zero (see bottom panel in Fig. 3), the electron is strongly accelerated by the residual ion and can gain enough energy

through non-elastic scattering to ionize. In Fig. 5 linear fits to  $v_z$  (in analogy to the green line in the bottom panel of Fig. 3) are shown for different ionization times in the central cycle at a fixed intensity, wavelength and initial transverse velocity. The linear fits are plotted for different pulse durations, which are chosen in each case as the maximal pulse duration,  $N_{max}$ , that will still lead to a Rydberg state, meaning one optical cycle more would cause a strong Coulomb interaction that accelerates the electron such that it will not be captured in a Rydberg state. From Fig. 5 we can see that the different ionization times mainly affect the slope of these lines but both the offset and the range of  $v_z$ ,  $\Delta v_z$ , are almost constant with variations below 1% for the offset and below 15% for  $\Delta v_z$  from the respective mean value. We therefore approximate as follows,

$$\Delta v_z \approx \text{const} = d(t_{0,max}) \cdot N_{max}, \quad (11)$$

where  $d$  is the slope of  $v_z$ . Furthermore, we find numerically for the dependence of  $t_{0,max}$  on the slope  $d$  that we can fit it nicely to a function

$$t_{0,max} = p \cdot d^\beta + q \quad (12)$$

with fitting parameters  $p$ ,  $q$ , and  $\beta$  (Fig. 6). In particular, we find about the same value for  $\beta$  for the different laser parameter sets shown in Fig. 6:  $\beta \approx 0.6$ .

How can we understand this result? As has been already discussed in section III, the electron is, on cycle average, exposed to an approximately constant force that pulls it closer to the ion. This Coulomb force is represented as the slope  $d$  in eq. 11 and it obviously depends on how far the electron is away from the ion on average. The drift momentum imposed by the laser field is  $\mathcal{E}_0/\omega \cdot \sin(\omega t_0) \approx \mathcal{E}_0 t_0$  and can be used as a quantifier for how far away from the residual ion the electron is pushed in the cycle average. So, the Coulomb force can be assumed to scale like  $-1/t_0^2$  with the ionization time, meaning  $d \propto 1/t_0^2$ . This seems to contradict our finding of  $d \propto t_{0,max}^{1/0.6} \approx t_{0,max}^2$  from the fit at first glance. However, as one can understand by the sketch in the inset of Fig. 6, the approximate  $1/t_0^2$  drop of the Coulomb force can be approximated around the typical values of  $t_0$  by a function that looks like a parabola  $t_0^2$ .

With the fitting result of eq. (12) we can conclude

$$R \propto (t_{0,max} - t_{0,min}) \propto d^\beta \propto \left(\frac{\Delta v_z}{N}\right)^\beta \propto N^{-\beta}. \quad (13)$$

The result obtained from the fit of  $\beta \approx 0.6$  compares well with the results from independent CTMC simulations, which give  $b \approx -0.5$  for all laser parameter sets displayed in Fig. 4, thereby identifying the mechanism behind the Rydberg ratio decreasing with pulse duration: Electrons that are born closer to the center of the pulse  $t_0 = 0$  experience a smaller drift momentum by the laser field and thus are - on average - closer to the residual ion, experience a stronger Coulomb force and are consequently driven back to the residual ion in less optical

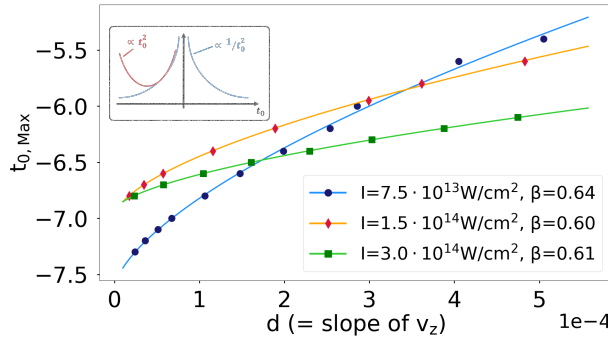


FIG. 6. The markers represent slopes of the linear fits to the minima of  $v_z$  for ionization from hydrogen in a laser with a wavelength of  $\lambda = 800\text{nm}$  for ionization at an initial transverse velocity of  $v_{t,0} = 0.15$  versus the maximal ionization time that still lead to the electron ending up in a Rydberg state for different intensities specified in the legend. The solid lines represent the corresponding fit of eq. (12) with the crucial fitting parameter  $\beta$  given in the legend.

cycles than electrons born earlier. Therefore electrons born at ionization times closer to  $t_0 = 0$  can be a Rydberg state only for shorter pulse durations.

## V. SUMMARY AND CONCLUSION

Using CTMC simulations we found that an increase of the pulse duration of the laser shifts the principle quantum number  $n$  of Rydberg states to larger values and that this increase scales approximately like the square root of the pulse duration. We could understand this result by finding that a typical trajectory that ends up in a Rydberg state has an approximately linear drift in its velocity along the laser polarization axis. Therefore the electron's cycle-averaged position is moving on a parabola, increasing its distance to the residual ion in the first part of the propagation and later approaching it again. In case the propagation in the laser field is so long that the electron gets so close to the parent ion that the strong interaction causes a significant acceleration, then the electron does not end up in a Rydberg state anymore. We found that electrons ending up in Rydberg states of small quantum numbers return to the parent ion more quickly and are thus 'scattered out' already for shorter pulse durations. A longer pulse duration thus leads to scattering out of more and more of the Rydberg states with a small principle quantum number  $n$  with an increasing boundary  $n_{min}$  where  $n > n_{min}$  still end up in a Rydberg state. This explains the shift of the quantum number distribution to larger quantum numbers.

Moreover, we observed a decrease of the fraction of electrons that end up in a Rydberg state with increasing pulse duration. We could understand this qualitatively and quantitatively again by the reduction of initial conditions ( $t_0, v_{t,0}$ ) that lead to Rydberg states with increasing pulse duration.

As the mechanisms that explain the pulse duration dependence stand in contrast to the mechanism found in a model that neglects the Coulomb force during the propagation in the laser field, the results presented here show that the Coulomb force has important consequences for quantum number distribution of Rydberg states. These insights allow for control of quantum number distributions via the pulse duration and will prove helpful in studies and applications that are based on the quantum number distribution of Rydberg atoms [7, 8, 12–14].

## Appendix A: Understanding the linear growth of the minima of $v_z$ with propagation time

If the electron were driven merely by the laser field and were not influenced by the Coulomb potential, then the velocity of the electron as a function of the time  $t$  after the ionization event would be given by

$$v_z(t) = -\frac{\mathcal{E}_0}{\omega}(\sin(\omega(t + t_0)) - \sin(\omega t_0)) \quad (\text{A1})$$

for a constant envelope (see sec. III for a justification of the constant envelope assumption). This function oscillates around the mean value of  $\mathcal{E}_0/\omega \cdot \sin(\omega t_0)$ , which can be approximated by  $\mathcal{E}_0 t_0$  and is thus negative for ionization times before the peak of the optical cycle, as it is typically the case for Rydberg states. This negative offset explains why the electron is initially slightly driven away from the residual ion (see center panel of Fig. 3).

Now, as one can see in the central panel of Fig. 3, even though the change of the 'mean' value - the position of the electron in  $z$ -direction that the electron oscillates around - is vital in the understanding of the electron's return, it changes rather slowly. Consequently, as the Coulomb force merely depends on the electron's position, the Coulomb force averaged over one optical cycle also does not change quickly and can be considered almost constant. A constant force, which is proportional to a constant acceleration, then leads to a linear change in the velocity, which is what we observe numerically (see bottom panel of Fig. 3).

## Appendix B: Understanding $N_{max} \propto z_{max}$

In this section we try to understand why we find numerically that the maximal number of optical cycles  $N_{max}$  that the pulse can have for a specific initial condition so that the electron still ends up in a Rydberg state depends linearly on the maximal elongation  $z_{max}$  of the parabola that we fit to the  $z(t)$  curve.

We now assume that the 'parabola' which  $z$  oscillates around returns to about  $z = 0$  after propagating  $N_{max}/2$  cycles, which should become clear by Fig. 3 and 7 and by the fact that for  $z$  close to zero the recollision is increasingly likely (note that we assume that the electron is born in the central cycle and that thus the pulse is on

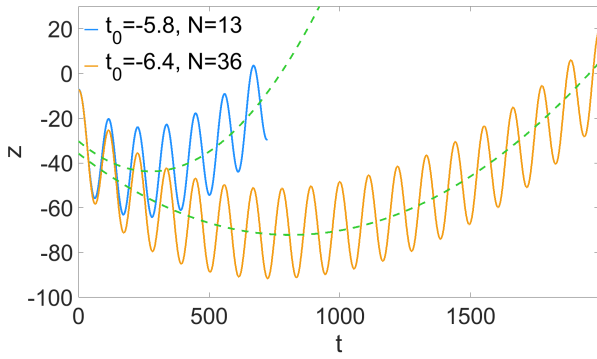


FIG. 7.  $z$  vs. propagation time  $t$  for trajectories ionized from hydrogen in a laser field of an intensity  $I = 1.5 \cdot 10^{14} \text{ W/cm}^2$  and a wavelength  $\lambda = 800\text{nm}$  with an initial transverse velocity  $v_{t,0} = 0.15$  for two different ionization times  $t_0$  and correspondingly two different pulse durations, which are chosen such that a pulse duration of one optical cycle more would have led to electron not ending up in a Rydberg state anymore. The dashed lines show a parabolic fit through the value that  $z$  oscillates around.

only for about  $N_{max}/2$  cycles after ionization). In Fig. 7 we see that the maximal value  $z_{max}$  occurs after a propagation time of about  $N_{max}/4$ . If we define the parabola fit function as  $z_{fit}(t) = d \cdot (e - t)^2 + f$  with fitting parameters  $d$ ,  $e$  and  $f$ , then we realize that  $e \approx N_{max}/4$  and  $f \approx z_{max}$ . So, mathematically the question is why we find approximately  $e \propto f$ . As we can see in Fig. 7, the parabolas for different  $t_0$  are very similar directly after ionization because the field strength at the time of birth is almost constant for the range of  $t_0$  that potentially end up in a Rydberg state. In terms of the fit function, we can write

$$\begin{aligned} z_{fit}(0) &= de^2 + f = P_1 \approx \text{const} \\ z'_{fit}(0) &= -2de = P_2 \approx \text{const} \end{aligned} \quad (\text{B1})$$

and thus it follows

$$\begin{aligned} f &= P_1 - de^2 = P_1 + P_2/2 \cdot e \\ \Rightarrow f &\propto e, \end{aligned} \quad (\text{B2})$$

which is what we observe numerically. So, we see that physically the discussed proportionality is due to very similar initial behavior of the parabolas due to the almost constant initial field for the small range of ionization times for which the electron can end up in a Rydberg state.

### Appendix C: Approximating the Rydberg area as a rectangle

In this section we want to briefly explain why the crescent shaped Rydberg area (see Fig. 2) is approximated as an rectangle in section IV the area of which is assumed to scale linearly with  $\Delta v$  and  $\Delta t$ . To this end, it

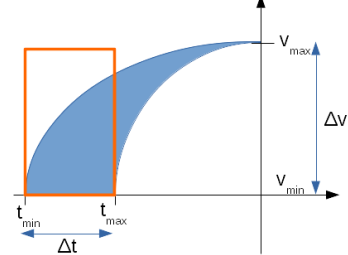


FIG. 8. Approximation of ellipse intersection as rectangle.

is instructive to look at the sketch in Fig. 8, where the crescent shaped area is approximated by the intersection of two ellipses of same height but different widths. As the following calculation shows the size of the intersection of the two ellipses (blue area) is about the area of the orange rectangle:

$$\begin{aligned} A_{\text{crescent}} &= \frac{1}{4} (A_{\text{large ellipse}} - A_{\text{small ellipse}}) \\ &= \frac{1}{4} |\pi \cdot \Delta v \cdot t_{min} - \pi \cdot \Delta v \cdot t_{max}| \\ &= \frac{\pi}{4} \cdot \Delta t \cdot \Delta v \approx A_{\text{rectangle}} \end{aligned} \quad (\text{C1})$$

In particular, this shows how the size of the Rydberg area scales linearly with  $\Delta t$ .

---

[1] L. Keldysh et al., Sov. Phys. JETP **20**, 1307 (1965).  
[2] P. B. Corkum, Physical Review Letters **71**, 1994 (1993).  
[3] M. Y. Ivanov, M. Spanner, and O. Smirnova, Journal of Modern Optics **52**, 165 (2005).  
[4] T. Nubbemeyer, K. Gorling, A. Saenz, U. Eichmann, and W. Sandner, Physical Review Letters **101**, 233001 (2008).  
[5] N. Shvetsov-Shilovski, S. Goreslavski, S. Popruzhenko, and W. Becker, Laser physics **19**, 1550 (2009).  
[6] B. Walker, B. Sheehy, L. F. DiMauro, P. Agostini, K. J. Schafer, and K. C. Kulander, Physical Review Letters **73**, 1227 (1994).  
[7] S. Eilzer and U. Eichmann, Journal of Physics B: Atomic, Molecular and Optical Physics **47**, 204014 (2014).  
[8] U. Eichmann, A. Saenz, S. Eilzer, T. Nubbemeyer, and W. Sandner, Physical Review Letters **110**, 203002 (2013).  
[9] L. Ortmann, C. Hofmann, and A. Landsman, Physical Review A **98**, 033415 (2018).  
[10] E. Wells, I. Ben-Itzhak, and R. Jones, Physical Review Letters **93**, 023001 (2004).  
[11] U. Eichmann, T. Nubbemeyer, H. Rottke, and W. Sandner, Nature **461**, 1261 (2009).

- [12] Q. Li, X.-M. Tong, T. Morishita, C. Jin, H. Wei, and C. Lin, *Journal of Physics B: Atomic, Molecular and Optical Physics* **47**, 204019 (2014).
- [13] H. Zimmermann, S. Patchkovskii, M. Ivanov, and U. Eichmann, *Physical Review Letters* **118**, 013003 (2017).
- [14] H. Zimmermann, S. Meise, A. Khujakulov, A. Magaña, A. Saenz, and U. Eichmann, *Physical Review Letters* **120**, 123202 (2018).
- [15] I. Burenkov, A. Popov, O. Tikhonova, and E. Volkova, *Laser Physics Letters* **7**, 409 (2010).
- [16] E. Volkova, A. Popov, and O. Tikhonova, *Journal of Experimental and Theoretical Physics* **113**, 394 (2011).
- [17] M. V. Fedorov, N. P. Poluektov, A. M. Popov, O. V. Tikhonova, V. Y. Kharin, and E. A. Volkova, *IEEE Journal of Selected Topics in Quantum Electronics* **18**, 42 (2012).
- [18] Q. Li, X.-M. Tong, T. Morishita, H. Wei, and C. D. Lin, *Physical Review A* **89**, 023421 (2014).
- [19] S. Popruzhenko, *Journal of Physics B: Atomic, Molecular and Optical Physics* **51**, 014002 (2017).
- [20] B. Zhang, W. Chen, and Z. Zhao, *Physical Review A* **90**, 023409 (2014).
- [21] H. Liu, Y. Liu, L. Fu, G. Xin, D. Ye, J. Liu, X. He, Y. Yang, X. Liu, Y. Deng, et al., *Physical Review Letters* **109**, 093001 (2012).
- [22] A. Landsman, A. Pfeiffer, C. Hofmann, M. Smolarski, C. Cirelli, and U. Keller, *New Journal of Physics* **15**, 013001 (2013).
- [23] W.-H. Xiong, X.-R. Xiao, L.-Y. Peng, and Q. Gong, *Physical Review A* **94**, 013417 (2016).
- [24] N. Delone and V. P. Krainov, *JOSA B* **8**, 1207 (1991).
- [25] M. V. Ammosov, N. B. Delone, and V. P. Krainov, *Sov. Phys. JETP* **64** (1986).
- [26] C. Hofmann, A. S. Landsman, C. Cirelli, A. N. Pfeiffer, and U. Keller, *Journal of Physics B: Atomic, Molecular and Optical Physics* **46**, 125601 (2013).
- [27] A. N. Pfeiffer, C. Cirelli, M. Smolarski, D. Dimitrovski, M. Abu-Samha, L. B. Madsen, and U. Keller, *Nature Physics* **8**, 76 (2012).
- [28] L.-B. Fu, J. Liu, J. Chen, and S.-G. Chen, *Physical Review A* **63**, 043416 (2001).
- [29] L. D. Landau and E. M. Lifshitz, *Quantum mechanics: non-relativistic theory*, vol. 3 (Elsevier, 2013).